Impact of the attenuation map on absolute and relative quantitation in 3D brain PET imaging: assessment of 6 different methods

Habib Zaidi, Marie-Louise Montandon and Daniel O Slosman

Abstract-- **The aim of this study is to compare the effect of the two major classes for determining the attenuation map, i.e. non-uniform versus uniform using clinical studies based on qualitative assessment as well as absolute and relative quantitative volume of interest (VOI)-based analysis. We investigate the effect of six different methods for determining patient-specific attenuation map: 2 approximate calculated methods, 2 TX-based methods, our newly developed segmented magnetic resonance imaging (MRI)-guided method, and finally an inferred anatomy-based technique. Ten cerebral clinical studies were selected from the database and used for clinical evaluation of the attenuation correction techniques. Several image quality parameters were compared including absolute and relative quantification indexes and correlation between them checked. The qualitative assessment showed no significant differences between the different attenuation correction techniques as assessed by expert physicians except the calculated automatic method, which generates artefacts in the upper edges of the head. Nevertheless, ANOVA results showed statistically significant differences between the different methods for some regions of the brain. The attenuation map influences both absolute and relative quantitation in cerebral 3D PET.**

I. Introduction

ATTENUATION correction is a crucial step both in qualitative assessment and quantitative analysis of reconstructed Positron Emission Tomography (PET) images. Information about patient-specific tissue attenuating properties can be derived from different methods, but is more commonly estimated by acquiring an additional pre-injection transmission (TX) scan using external sources. While the clinical relevance of non-uniform attenuation correction is well established in thoracic imaging, it is still the subject of heated debate in brain scanning [1, 2]. Brain PET studies simplify this task owing to the homogeneous characteristics of tissue components in the head region. This fact has motivated the development of approximate methods to correct for attenuation with the aim to partially minimize some of the side effects described above. Calculated methods are at the top of this simplification scheme.

This work was supported by the Swiss National Science Foundation under grant SNSF 3152-062008.

The authors are with the division of nuclear medicine, Geneva University Hospital, Geneva 1211, Switzerland (telephone: +41 22 372 7258, e-mail: habib.zaidi@hcuge.ch).

It is generally well accepted that TX-based non-uniform attenuation correction (AC) can supply more accurate absolute quantification; however, it is not entirely clear whether it provides precise benefits in the routine clinical practice of brain 3D positron PET imaging. The aim of this study is to compare the effect of six different methods belonging the two major classes for determining the attenuation map, i.e. non-uniform versus uniform, using clinical 3D brain PET studies based on qualitative assessment as well as absolute and relative quantitative volume of interest (VOI)-based analysis.

II. Materials and Methods

A. Methods for determination of the attenuation map

We investigate the effect of six different methods for determining patient-specific attenuation map: 2 approximate calculated methods, 2 TX-based methods, our newly developed segmented magnetic resonance imaging (MRI)-guided method [3], and finally an inferred anatomy-based technique [4]. The first calculated method refereed to as uniform fit-ellipse method (UFEM) approximates the outline of the head by an ellipse assuming a constant linear attenuation factor ($\mu = 0.096 cm^{-1}$) for soft tissue; while the second refereed to as automated contour detection method (ACDM), estimates the outline of the head from the emission sinogram [5]. Attenuation of the skull is accounted for by assuming a certain uniform skull thickness ($0.45\ cm^{-1}$) within the estimated shape and the correct μ value ($0.151\ cm^{-1}$) is used. The usual measured transmission method using ^{137}Cs single-photon sources was used instead without (MTM) and with segmentation of the TX data (STM). Those techniques are finally compared to the segmented MRI method (SMM), [3] and to an implementation of the inferring attenuation distributions method (IADM) based on the digital Zubal head atlas [4].

B. Clinical data acquisition and reconstruction

A total of ten patients were randomly selected from our clinical database and used for comparative assessment of different attenuation correction techniques. Selection was restricted to patients who previously underwent a brain MRI scan. The emission study (25 min) started 30 min after

intravenous injection of approximately 222 MBq of [^{18}F]-Fluorodeoxyglucose (FDG). All data sets were acquired in 3D mode with a maximum acceptance angle corresponding to 17 rings and a span of 7 on the ECAT ART PET scanner (CTI PET Systems, Knoxville, TN, USA) upgraded to use collimated ^{137}Cs single-photon point sources for TX scanning. Acquired projection data were pre-corrected for scatter using the latest numerical implementation of the single-scatter simulation algorithm [6]. Attenuation correction factors were generated by forward projecting the constructed attenuation maps obtained using the six different methods described in the previous section without any extra smoothing. The reprojection algorithm (3DRP) [7], used routinely in clinical brain studies at our division was used for image reconstruction (Ramp filter, cut-off frequency 0.35 cycles/pixel).

Patients' anatomy was defined using high-resolution 3D T1-weighted MR sequence performed on a 1.5-Tesla Eclipse scanner (Philips Medical Systems, Best, The Netherlands). A three-dimensional volumetric acquisition of a T1-weighted gradient echo sequence produced a gapless series of thin sagittal sections using a magnetization preparation rapid acquisition gradient-echo sequence (TE/TR, 4.4/15 ms; flip angle, 25°; acquisition matrix, 256*x*256*x*160; slice thickness, 1.1 mm).

C. Comparative evaluation strategy

Qualitative and quantitative assessments of differences between reconstructed using different attenuation correction methods were performed by visual assessment performed by expert physicians and by estimating parameters of clinical interest including absolute and relative regional cerebral glucose metabolism (rCGM). Several image quality parameters were compared including absolute and relative quantification indexes and correlation between them checked. Statistical analysis was also performed to assess the significance of the differences.

Template-based quantification is a crucial step when performing comparative evaluation of quantitative measurements. T1-weighted MRI template provided within the Statistical Parametric Mapping (SPM99) software package (Wellcome Department of Cognitive Neurology, University College London, London, U.K) was used to delineate manually a total of 20 bilateral volumes of interest (VOIs) covering the totality of cortical and subcortical structures. These were transformed to the coordinate space of the PET images to quantify FDG uptake. PET and MRI templates come already spatially normalized with respect to each other, and therefore it was found convenient to register the reconstructed images with respect to the PET template. The images were realigned to the standardized stereotactic template using a nine-parameter rigid body transformation for automated VOI quantification.

In this study, rCGM for each VOI was normalized to mean cerebellar rCGM estimates. The normalization constant was taken as the mean left and right rCGM. Cerebellar normalization is commonly reported in studies dealing with Alzheimer's disease and receptor imaging. The contrast between the corpus callosum and lateral ventricle and

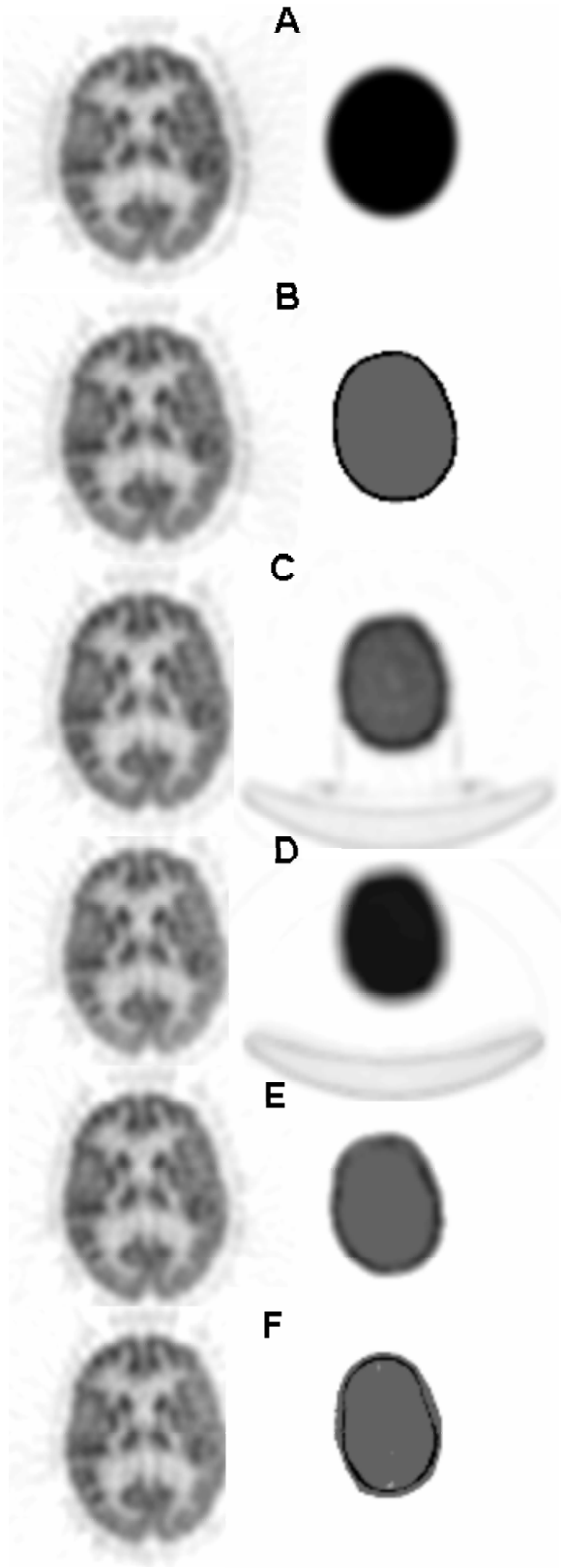

Fig. 1. Transaxial slice of 3DRP reconstructions of clinical 3D brain PET images (left) and attenuation maps used for attenuation correction (right). **A.** UFEM, **B.** ACDM, **C.** MTM, **D.** STM, **E.** SMM, and finally **F.** IADM.

uniformity within the cerebellum was also compared between the different methods. One way repeated ANOVA was used to test significant quantitation differences in rCGM for each VOI when applying the different AC methods under investigation.

III. Results

A. Qualitative assessment

Representative plane of 3DRP filtered backprojection reconstructions together with attenuation maps generated using the different methods for a clinical brain PET study are shown in Fig. 1. From a purely qualitative analysis, the merits of the more exact methods based on realistic nonuniform attenuation maps are obvious. They produce less visible artifacts, while the approximate methods tend to produce an artifact in which there is a high level of activity along the edge of the image due to overestimation of the head contour when using the ACDM on the external slices.

B. Quantitative evaluation

The quantitative VOI-based analysis revealed different performance and statistically significant differences between the different correction techniques when compared to the gold standard (MTM). Fig. 2 shows linear regression plots illustrating correlation between MTM and other attenuation correction algorithms.Correlation in mean rCGM values with respect to the gold standard (MTM) was good, except for ACDM (R^2=0.54). The STM and SMM methods showed the best correlation (R^2=0.9) and the regression lines agreed well with the line of identity. The results of the statistical comparison between rCGM estimates when using the different attenuation and correction techniques is summarized in table I. Overall, individual VOI standard deviations were significantly smaller for calculated and segmented-based attenuation correction algorithm compared to MTM. The percent differences between the correction techniques are minor but statistically significant for some regions whereas no proof of statistically significant differences could be verified for the other regions. The number of VOIs showing a high probability of a true difference increased substantially after normalization to the cerebellum for all methods except IADM. Nevertheless, higher correlation coefficients were obtained on semi-quantitative estimates.

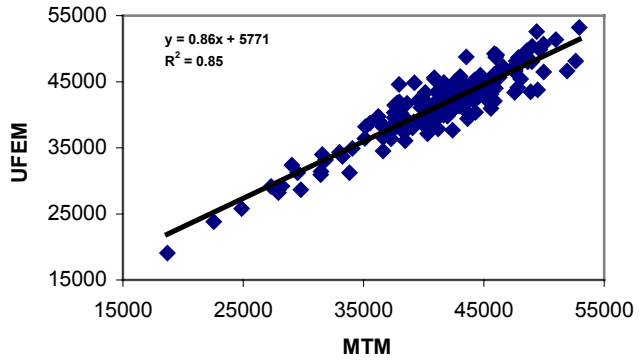

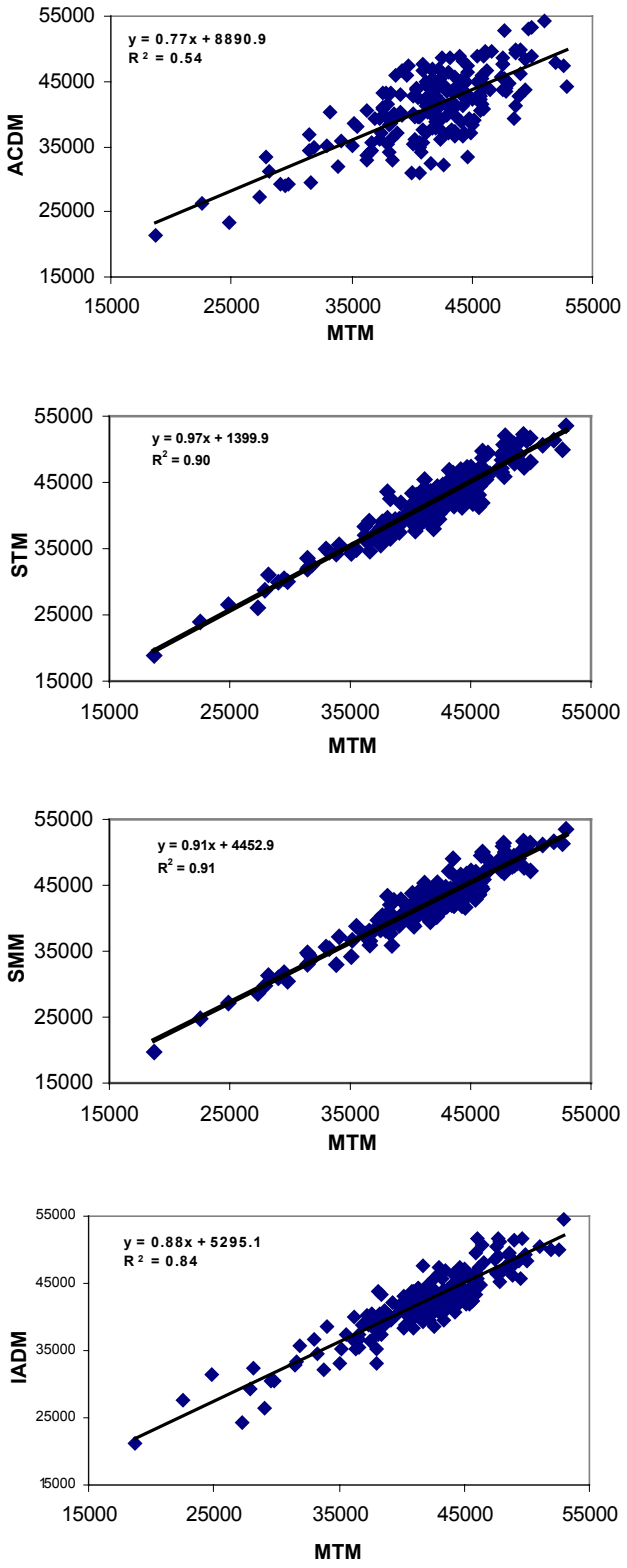

Fig 2. Correlation plots between mean rCGM values obtained from reconstructions of clinical 3D brain scans guided by measured transmission and alternative attenuation correction methods. A total of two hundred data points (10 patients and 20 VOIs) are shown. From top to bottom: UFEM and MTM, ACDM and MTM, STM and MTM, SMM and MTM, and finally IADM and MTM. Correlation coefficients and best fit equations are also shown.

TABLE I
SUMMARY OF STATISTICAL ASSESSMENT USING REPEATED ANOVA ANALYSIS FOR COMPARING ABSOLUTE rCGM ESTIMATES OBTAINED FROM CLINICAL BRAIN PET RECONSTRUCTIONS CORRECTED FOR ATTENUATION USING THE 5 DIFFERENT ATTENUATION MAPS AS COMPARED TO RECONSTRUCTIONS GUIDED BY MEASURED TRANSMISSION, WHICH SERVED AS GOLD STANDARD.

VOI	UFEM	ACDM	STM	SMM	IADM
LFL	0.499	0.017	0.652	0.502	0.160
RFL	0.078	0.057	0.659	0.191	0.123
LPL	0.621	0.037	0.115	0.413	0.518
RPL	0.108	0.039	0.318	0.323	0.213
LTL	0.101	0.342	0.300	0.154	0.608
RTL	0.139	0.868	0.076	0.488	0.794
LOL	0.155	0.082	0.002*	0.008	0.047
ROL	0.068	0.145	0.002*	0.517	0.323
LC	0.011	0.178	0.613	0.020	0.336
RC	0.036	0.137	0.271	0.007	0.118
CG	0.708	0.562	0.068	0.222	0.965
P	0.469	0.032	0.003*	0.001*	0.135
LT	0.110	0.499	0.003*	0.002*	0.023
RT	0.047	0.137	0.005*	<0.001*	0.002*
LP	0.622	0.464	0.051	0.190	0.605
RP	0.266	0.611	0.027	0.037	0.087
LH	0.316	0.422	0.982	0.454	0.478
RH	0.417	0.313	0.374	0.092	0.304
LHCN	0.157	0.177	0.114	0.053	0.864
RHCN	0.871	0.197	0.004*	0.009	0.028

Figs. 3 and 4 illustrate Box-and-Whisker plot for contrast assessment between the corpus callosum and the lateral ventricle and uniformity assessment in the cerebellum when using the different attenuation correction techniques, respectively. The analysis of contrast assessment between the corpus callosum and the lateral ventricle when using different attenuation correction schemes revealed significantly lower estimates when using MTM and STM, the former being noisier than all other methods. No significant differences were noticed on uniformity assessment when using the different attenuation correction schemes investigated in this study.

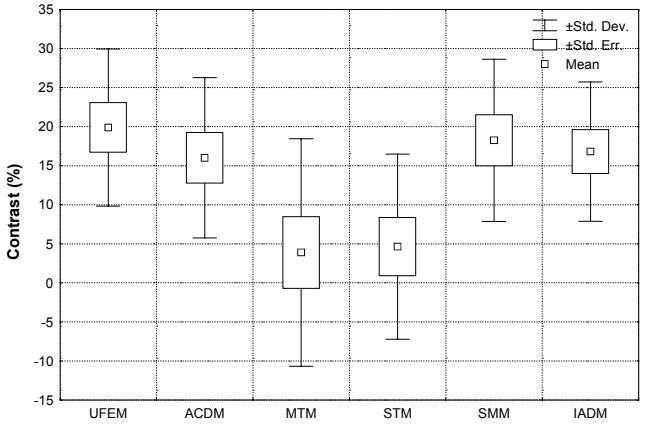

Fig 3. Box-and-Whisker plot for contrast assessment between the corpus callosum and the lateral ventricle when using different attenuation correction schemes.

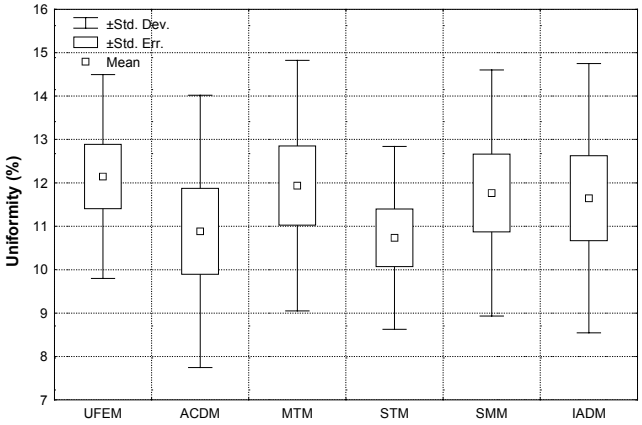

Fig 4. Box-and-Whisker plot for uniformity assessment in the cerebellum when using the different attenuation correction techniques.

IV. DISCUSSION AND CONCLUSION

The challenging issue in assessing differences between the effectiveness of uniform versus non-uniform attenuation maps have been largely studied in SPECT. However, very few studies have been performed to characterize them using PET data. The attenuation map influences both absolute and relative quantitation in cerebral 3D PET. The quantitative VOI-based analysis revealed different performance and statistically significant differences between the different correction techniques when compared to the gold standard (MTM). Transmissionless attenuation correction results in reduced radiation dose and makes a dramatic difference in acquisition time allowing increased patient throughput. The necessity of acquiring an additional TX scan is a restrictive factor for patient throughput. Considering the difficulties associated with TX-based attenuation correction and the limitations of current calculated attenuation correction, MRI-based attenuation correction in 3D brain PET would likely be the method of choice for the foreseeable future as a second best approach in a busy PET facility and could be applied to other functional brain imaging modalities (e.g. SPECT).

V. REFERENCES

[1] K. Van Laere, M. Koole, J. Versijpt, and R. Dierckx, "Non-uniform versus uniform attenuation correction in brain perfusion SPET of healthy volunteers," *Eur J Nucl Med*, vol. 28, pp. 90-98, 2001.

[2] H. Zaidi and B. H. Hasegawa, "Determination of the attenuation map in emission tomography," *J Nucl Med*, vol. 44, pp. 291-315, 2003.

[3] H. Zaidi, M.-L. Montandon, and D. O. Slosman, "Magnetic resonance imaging-guided attenuation and scatter corrections in 3D brain positron emission tomography," *Med Phys*, vol. 30, pp. 937-948, 2003.

[4] R. Z. Stodilka *et al*, "Scatter and attenuation correction for brain SPECT using attenuation distributions inferred from a head atlas," *J Nucl Med*, vol. 41, pp. 1569-1578, 2000.

[5] M. Bergstrom, J. Litton, L. Eriksson, C. Bohm, and G. Blomqvist, "Determination of object contour from projections for attenuation correction in cranial positron emission tomography," *J Comput Assist Tomogr*, vol. 6, pp. 365-372, 1982.

[6] C. C. Watson, "New, faster, image-based scatter correction for 3D PET," *IEEE Trans Nucl Sci*, vol. 47, pp. 1587-1594, 2000.

[7] P. E. Kinahan and J. G. Rogers, "Analytic 3D image reconstruction using all detected events," *IEEE Trans Nucl Sci*, vol. 36, pp. 964-968, 1989.

* Regions showing highest probability of a true difference.